Geomechanics and Engineering, Vol. 3, No. 4 (2011) 255-266
DOI: http://dx.doi.org/10.12989/gae.2011.3.4.255

Pseudo-dynamic approach of seismic earth pressure behind cantilever retaining wall with inclined backfill surface

Debabrata Giri*

Department of Civil Engineering, Parala Maharaja Engineering College, Berhampur, BPUT University, Odisha, India

(Received March 5, 2011, Revised November 14, 2011, Accepted November 16, 2011)

Abstract. Knowledge of seismic earth pressure against rigid retaining wall is very important. Mononobe-Okabe method is commonly used, which considers pseudo-static approach. In this paper, the pseudo-dynamic method is used to compute the distribution of seismic earth pressure on a rigid cantilever retaining wall supporting dry cohesionless backfill. Planar rupture surface is considered in the analysis. Effect of various parameters like wall friction angle, soil friction angle, shear wave velocity, primary wave velocity, horizontal and vertical seismic accelerations on seismic earth pressure have been studied. Results are presented in terms of tabular and graphical non-dimensional form.

Keywords: seismic earth pressure; retaining wall; Mononobe-Okabe method; pseudo-static approach; pseudo-dynamic method; seismic acceleration.

1. Introduction

The concept of earth pressure under both static and seismic condition is very important in designing a retaining wall as the damage of such structures may lead to catastrophic failure. Many researchers have developed several methods to determine the seismic earth pressure against a rigid retaining wall. Okabe (1926) and Mononobe and Matsuo (1926) provided data related to active and passive earth pressure using pseudo-static analysis. This method was later recognized as Mononobe-Okabe method, which is the modification of Coulomb approach. Using upper bound limit analysis, Soubra (2000) determined both static and seismic passive earth pressure by considering the multi-block mechanism. Saran and Gupta (2003), Ghosh *et al.* (2008), Ghosh (2010), Ghosh and Saran (2010) considered pseudo-static approach to compute the seismic active earth pressure behind a retaining wall. In pseudo-static approach, the dynamic loading induced by earthquake is considered as time independent, which ultimately reduced to constant magnitude and phase acceleration throughout the backfill. To overcome this constraint, Steedman and Zeng (1990) presented pseudo-dynamic approach to predict the seismic active earth pressure behind a vertical retaining wall. Further, extension of this approach is done by Choudhury and Nimbalkar (2005), Choudhury and Nimbalkar (2006) to evaluate

*Ph.D., E-mail: debagiri@gmail.com

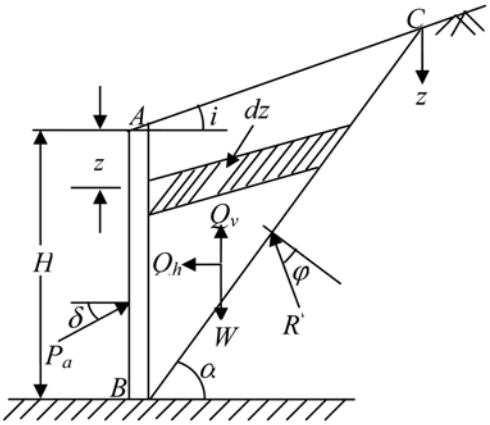

Fig. 1 Failure mechanism and associated forces

seismic passive and active earth pressure behind a vertical retaining wall. Ghosh (2007) extended the Choudhury and Nimbalkar (2005) approach to consider the inclination of retaining wall to evaluate seismic passive earth pressure. The present study explores the effect of wall friction angle, δ, soil friction angle, φ, coefficient of horizontal as well as vertical earthquake force, k_h, k_v and inclination of backfill, i on the seismic active earth pressure using the pseudo-dynamic approach. Limit equilibrium method, with a planar failure surface behind the retaining wall has been considered to compute the earth pressure against wall.

2. Definition of the problem

A rigid vertical cantilever retaining wall of height H is placed with dry cohesionless, inclined back fill as shown in Fig. 1. The wall friction angle is inclined at an angle, δ, with the horizontal. The objective of present study is to determine the active earth pressure coefficients and distribution by knowing the total active pressure resistance P_{ae} per unit length of the wall in the presence of both horizontal and vertical earthquake acceleration $k_h g$ and $k_v g$ respectively, where g is the acceleration due to gravity. The effects of soil friction, φ, wall friction angle, δ, and backfill surface inclination, i, on the normalized active seismic earth pressure are studied and are represented in both tabular and graphical forms. The parameters shown in Fig. 1 are positive and unit weight of back fill soil is taken as γ.

3. Method of analysis

The pseudo-dynamic analysis, which considers a finite shear wave velocity, can be developed by assuming that the shear modulus G, is constant with depth through the backfill and the phase and not the magnitude of acceleration varies. In the present study, both shear wave velocity, $V_s = \sqrt{G/\rho}$ and primary velocity $V_p = \sqrt{G(2-2\nu)/\rho(1-2\nu)}$ where ρ and ν are the density and poisson's ratio of the backfill material respectively, are assumed to act within the soil media due to earthquake loading. A planar rupture surface inclined at an angle α with the horizontal is considered in the

present analysis. The analysis includes a period of lateral shaking T, which can be expressed as $T = 2\pi/\omega$, where ω is the angular frequency.

For a sinusoidal base shaking subjected to both horizontal and vertical earthquake acceleration with amplitude $k_h g$ and $k_v g$, the acceleration at any depth z below the ground surface and time t can be expressed as

$$a_h(z,t) = k_h g \sin\omega\left(t - \frac{H-z}{V_s}\right) \tag{1}$$

$$a_v(z,t) = k_h g \sin\omega\left(t - \frac{H-z}{V_p}\right) \tag{2}$$

The mass of the small shaded part of thickness dz as shown in Fig. 1 is given by

$$m(z) = \frac{\gamma \cos\alpha (H-z)}{g \sin(\alpha - i)} dz \tag{3}$$

The total weight of the failure wedge W can be derived from the Eq. (3) and is given by

$$W = \frac{\gamma H^2 \cos\alpha}{2 \sin(\alpha - i)} \tag{4}$$

The horizontal inertia force exerted on the small element due to horizontal earthquake acceleration can be expressed as $m(z)a_h(z,t)$. Therefore the total horizontal inertia force $Q_h(t)$ acting on the failure wedge is given by

$$Q_h(t) = \int_0^H k_h g \sin\omega\left(t - \frac{H-z}{V_s}\right) \frac{\gamma \cos\alpha (H-z)}{g \sin(\alpha - i)} dz \tag{5}$$

On simplification the Eq. (5) becomes

$$Q_h(t) = \frac{k_h \gamma \lambda_s \cos\alpha}{4\pi^2 \sin(\alpha - i)} \left[2\pi H \cos 2\pi\left(\frac{t}{T} - \frac{H}{\lambda_s}\right) + \lambda_s \left\{ \sin 2\pi\left(\frac{t}{T} - \frac{H}{\lambda_s}\right) - \sin 2\pi\left(\frac{t}{T}\right) \right\} \right] \tag{6}$$

Where, λ_s is the wave length of shear wave. Similarly, the total vertical inertia force $Q_v(t)$ acting in the failure wedge is given by

$$Q_v(t) = \int_0^H k_v g \sin\omega\left(t - \frac{H-z}{V_p}\right) \frac{\gamma \cos\alpha (H-z)}{g \sin(\alpha - i)} dz \tag{7}$$

Which, can be simplified as

$$Q_v(t) = \frac{k_v \gamma \lambda_p \cos\alpha}{4\pi^2 \sin(\alpha - i)} \left[2\pi H \cos 2\pi\left(\frac{t}{T} - \frac{H}{\lambda_p}\right) + \lambda_p \left\{ \sin 2\pi\left(\frac{t}{T} - \frac{H}{\lambda_p}\right) - \sin 2\pi\left(\frac{t}{T}\right) \right\} \right] \tag{8}$$

Where, $\lambda_p = TV_p$ is the wave length of primary wave. The total active force $P_{ae}(t)$ can be computed by taking the horizontal as well as vertical equilibrium of the failure wedge and is given by

$$P_{ae}(t) = \frac{W\sin(\alpha-\varphi) + Q_h(t)\cos(\alpha-\varphi) - Q_v(t)\sin(\alpha-\varphi)}{\cos(\varphi+\delta-\alpha)} \tag{9}$$

The seismic active earth pressure coefficient $K_{ae}(t)$ is defined as

$$K_{ae}(t) = \frac{2P_{ae}(t)}{\gamma H^2} \tag{10}$$

Substituting for Q_h and Q_v in the Eq. (10), an expression for K_{ae} can be obtained as

$$K_{ae} = \frac{\cos\alpha\sin(\alpha-\varphi)}{\sin(\alpha-i)\cos(\delta+\varphi-\alpha)} + \frac{k_h\cos\alpha}{2\pi^2\sin(\alpha-i)}\left(\frac{TV_s}{H}\right)\frac{\cos(\alpha-\varphi)}{\cos(\delta+\varphi-\alpha)}\times C_1$$
$$- \frac{k_v\cos\alpha}{2\pi^2\sin(\alpha-i)}\left(\frac{TV_p}{H}\right)\frac{\cos(\alpha-\varphi)}{\cos(\delta+\varphi-\alpha)}\times C_2 \tag{11}$$

Where,

$$C_1 = \left[2\pi\cos 2\pi\left(\frac{t}{T}-\frac{H}{TV_s}\right) + \left(\frac{TV_s}{H}\right)\left(\sin\left(\frac{t}{T}-\frac{H}{TV_s}\right)-\sin\left(\frac{t}{T}\right)\right)\right]$$

$$C_2 = \left[2\pi\cos 2\pi\left(\frac{t}{T}-\frac{H}{TV_p}\right) + \left(\frac{TV_p}{H}\right)\left(\sin\left(\frac{t}{T}-\frac{H}{TV_p}\right)-\sin\left(\frac{t}{T}\right)\right)\right]$$

It can be observed from the Eq. (11) that $K_{ae}(t)$ is a function of α, t/T, H/λ_s and H/λ_p. H/λ_s is simply the ratio of time taken by the shear wave to travel the full height to the period of lateral shaking T. Similarly H/λ_p is the ratio of time taken by the primary wave to travel the full height for a shaking period T. For most of the geological materials V_p/V_s can be taken as 1.87 Das (1993). Therefore, to satisfy this relationship, the magnitude of H/λ_s and H/λ_p have been kept equal to 0.3 and 0.16 respectively throughout the analysis. The optimization has been done with respect to α and t/T to get the maximum value of $K_{ae}(t)$ and the optimum values are represented as K_{ae}. During optimization the value of α and t/T have been varied in the range of 0^0-90^0 and 0-1 respectively.

The active earth pressure distribution behind the retaining wall can be determined by taking partial derivative of $P_{ae}(z, t)$ with respect to z and expressed as

$$p_{ae}(z,t) = \frac{\partial P_{ae}(z,t)}{\partial z}$$
$$= \frac{\gamma z\cos\alpha\sin(\alpha-\varphi)}{\sin(\alpha-i)\cos(\delta+\varphi-\alpha)} + \frac{k_h\gamma z\cos\alpha}{\sin(\alpha-i)}\frac{\cos(\alpha-\varphi)}{\cos(\delta+\varphi-\alpha)}\sin\left[\omega\left(t-\frac{z}{V_s}\right)\right]$$
$$- \frac{k_v\gamma z\cos\alpha}{\sin(\alpha-i)}\frac{\sin(\alpha-\varphi)}{\cos(\delta+\varphi-\alpha)}\sin\left[\omega\left(t-\frac{z}{V_p}\right)\right] \tag{12}$$

This Eq. (12) is similar to that obtained by Choudhury *et al.* (2004) for the specific case of zero degree backfill inclination, i. The first term in the Eq. (12), represents the static earth pressure acting on the retaining wall. The second and third terms represent the dynamic earth pressure acting on retaining wall due to horizontal and vertical inertia of the soil wedge respectively.

4. Results and discussions

To avoid the phenomenon of shear fluidization for the cohesionless soils, for the certain combinations of k_h and k_v, the value of φ considered in the analysis are to satisfy the relationship as given by, Richards *et al.* (1990)

$$\varphi > \left(i + \tan^{-1} \frac{k_h}{1 - k_v} \right) \tag{13}$$

Results are presented in tabular and graphical form for normalized active seismic active earth

Table 1 Value of k_{ae} for k_h = 0.1, k_v = 0

φ (^{0})	δ (^{0})	Backfill surface angle in degree (i)		
		0	10	20
20	0	0.537931	0.483525	0.419681
	10	0.473557	0.420516	0.360155
	20	0.438953	0.385885	0.326844
30	0	0.513443	0.539336	0.599131
	10	0.482785	0.507973	0.568431
	20	0.471965	0.497036	0.559999
	30	0.478278	0.504028	0.571333
40	0	0.382624	0.389945	0.410916
	10	0.366760	0.373106	0.393290
	20	0.364294	0.369805	0.389809
	30	0.374615	0.379373	0.399736
	40	0.399855	0.403411	0.424921

Table 2 Value of k_{ae} for k_h =0.2, k_v = 0

φ (^{0})	δ (^{0})	Backfill surface angle in degree (i)		
		0	10	20
20	0	0.651903	0.646921	0.640775
	10	0.547747	0.542205	0.535761
	20	0.494397	0.488429	0.481638
30	0	0.462763	0.442709	0.419625
	10	0.429608	0.408826	0.38543
	20	0.415172	0.393158	0.368799
	30	0.416242	0.392035	0.365899
40	0	0.355859	0.3379	0.31701
	10	0.339201	0.320563	0.299286
	20	0.335235	0.315306	0.292971
	30	0.343122	0.321099	0.296802
	40	0.364483	0.338932	0.311525

pressure along the normalized depth of the retaining wall. Various parameters considered as follows:

$\varphi = 20^0, 30^0$ and 40^0 $\quad k_h = 0.0, 0.1, 0.2$ and 0.3
$\delta = 0^0, 10^0, 20^0, 30^0, 40^0$ $\quad k_v = 0.0k_h, 0.5k_h$ and k_h

The values of seismic active earth pressure coefficient, K_{ae} are given in Tables 1 to 7 for different values of k_h and k_v. From the tables, it is observed that the magnitude of the seismic active earth pressure coefficients are increasing with the increase in both horizontal and vertical accelerations for a particular value of soil friction angle and wall friction angle along a constant backfill inclination.

Table 3 Value of k_{ae} for $k_h = k_v = 0.1$

φ (^{0})	δ (^{0})	Backfill surface angle in degree (i)		
		0	10	20
20	0	0.700313	0.689518	0.676643
	10	0.592556	0.580241	0.566125
	20	0.537474	0.524061	0.508956
30	0	0.39289	0.382	0.369026
	10	0.361916	0.350621	0.337441
	20	0.347359	0.335392	0.321664
	30	0.345825	0.332736	0.317992
40	0	0.289691	0.280183	0.268691
	10	0.273936	0.26413	0.252472
	20	0.268632	0.258212	0.246024
	30	0.272733	0.261296	0.248088
	40	0.287019	0.273907	0.259071

Table 4 Value of k_{ae} for $k_h = k_v = 0.2$

φ (^{0})	δ (^{0})	Backfill surface angle in degree (i)		
		0	10	20
20	0	0.768797	0.74908	0.72639
	10	0.657199	0.63508	0.61052
	20	0.599524	0.57617	0.550274
30	0	0.461727	0.441752	0.418787
	10	0.428445	0.407675	0.384306
	20	0.413927	0.391861	0.367475
	30	0.414822	0.390613	0.364349
40	0	0.355378	0.337519	0.316769
	10	0.338625	0.320047	0.298863
	20	0.334566	0.314697	0.292432
	30	0.342367	0.320359	0.296101
	40	0.363631	0.338155	0.310646

Table 5 Value of k_{ae} for $k_v = 0.5\ k_h$, $k_h = 0.1$

$\varphi\ (^0)$	$\delta\ (^0)$	Backfill surface angle in degree (i)		
		0	10	20
20	0	0.7018	0.690896	0.677901
	10	0.595041	0.582888	0.569034
	20	0.540229	0.527122	0.512627
30	0	0.393669	0.382712	0.369658
	10	0.362871	0.351564	0.338381
	20	0.348462	0.336511	0.322821
	30	0.347068	0.334053	0.319385
40	0	0.290309	0.280622	0.268907
	10	0.274958	0.264975	0.253108
	20	0.270039	0.259463	0.24708
	30	0.274533	0.262956	0.249608
	40	0.289223	0.276008	0.261064

Table 6 Value of k_{ae} for $k_v = 0.5\ k_h$, $k_h = 0.2$

$\varphi\ (^0)$	$\delta\ (^0)$	Backfill surface angle in degree (i)		
		0	10	20
20	0	0.70341	0.692446	0.679402
	10	0.597591	0.585606	0.572104
	20	0.543012	0.53025	0.516298
30	0	0.394449	0.383465	0.370392
	10	0.363825	0.352535	0.33938
	20	0.349581	0.337676	0.324062
	30	0.348311	0.335386	0.320854
40	0	0.290206	0.280571	0.268892
	10	0.274679	0.264776	0.252979
	20	0.269615	0.259124	0.246827
	30	0.273908	0.26242	0.249177
	40	0.288456	0.275371	0.260495

4.1 Effect of k_h and k_v

The typical variation of normalized pressure distribution for different values of k_h with $k_v = 0.5k_h$, $\varphi = 30^0$, $\delta = \varphi/2$, $H/\lambda_s = 0.3$, $H/\lambda_p = 0.16$ and for a constant backfill inclination, $i = 20^0$ is shown in Fig. 2.

It is seen that as k_h increases, active earth pressure also increases. When k_h increases from 0.1 to 0.2, seismic active earth pressure increases by 32.55% at the bottom, 48.72% at the mid height of the wall. Similarly when k_h increases from 0.1 to 0.3, seismic active earth pressure increases by 36.79% at the bottom, 48.85% at the mid height of the wall. Degree of non-linearity of the curves

Table 7 Value of k_{ae} for $k_v = 0.5\ k_h$, $k_h = 0.3$

φ (^{0})	δ (^{0})	Backfill surface angle in degree (i)		
		0	10	20
20	0	0.754337	0.736737	0.716234
	10	0.644925	0.625607	0.604046
	20	0.588585	0.567878	0.545477
30	0	0.445741	0.428022	0.407505
	10	0.413233	0.394927	0.37417
	20	0.398901	0.379515	0.357926
	30	0.399324	0.378156	0.355002
40	0	0.339283	0.323482	0.304976
	10	0.322909	0.306564	0.287714
	20	0.318642	0.301232	0.281494
	30	0.32559	0.306381	0.28498
	40	0.345191	0.32307	0.298864

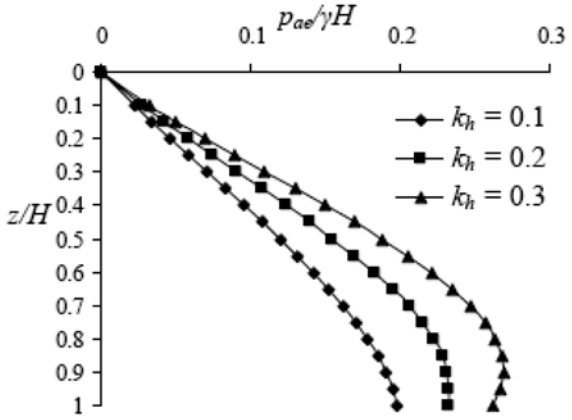

Fig. 2 Typical normalized active earth pressure distribution for different values of k_h with $k_v = 0.5k_h$

also increases for higher values of k_h.

4.2 Effect of soil friction angle (φ)

The normalized pressure distribution for different values of soil friction angle, φ with $k_v = 0.5k_h$, $k_h = 0.2$, $\delta = \varphi/2$, $H/\lambda_s = 0.3$, $H/\lambda_p = 0.16$ and for a constant backfill inclination, $i = 20^0$ is presented in Fig. 3.

Seismic active earth pressure shows significant decrease with increase in the value of soil friction angle. When φ increases from 20^0 to 30^0, seismic active earth pressure decreases by 22.67% at the bottom, 15.85% at the mid height of the wall. Similarly, when φ changes from 30^0 to 40^0, seismic active earth pressure decreases by about 13.7% at the bottom of the wall and 6.3% at the mid-

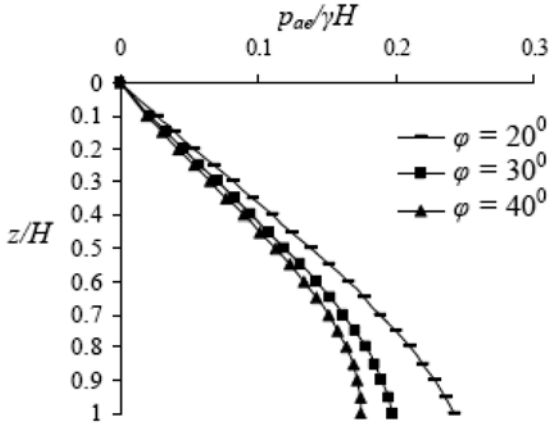

Fig. 3 Normalized active earth pressure distribution for different values of φ with $k_v = 0.5k_h$

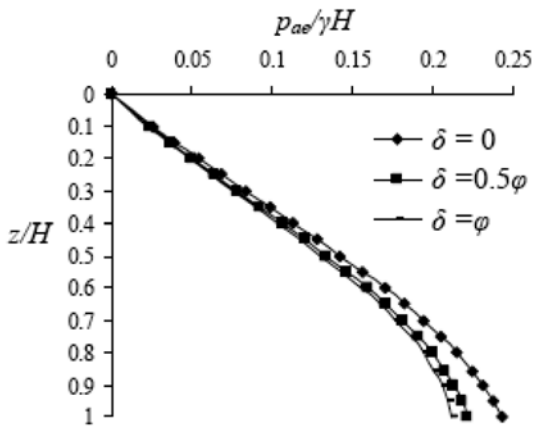

Fig. 4 Normalized seismic active earth pressure distribution for different values wall friction angle, δ, with $k_v = 0.5k_h$, $k_h = 0.2$ and $\varphi = 30^0$

height of the wall.

4.3 Effect of wall friction angle (δ)

Fig. 4 shows the normalized distribution of seismic active earth pressure for different values of wall friction angle, δ, with $k_v = 0.5k_h$, $k_h = 0.2$, $\varphi = 30^0$, $i = \varphi/2$, $H/\lambda_s = 0.3$, $H/\lambda_p = 0.16$.

Seismic active earth pressure shows relatively marginal decrease with the increase in wall friction angle, δ. As δ changes from 0 to 0.5φ: seismic active earth pressure decreases by about 9.1% at the base of the wall and about 6.4% at the mid height of the wall. Similarly, when δ increases from 0.5φ to φ, seismic active earth pressure decreases by about 4.2% at the base of the wall and about 2.2% at the mid height of the wall.

4.4 Effect of backfill surface inclination (i)

The variation of normalized seismic active earth pressure with respect to backfill surface inclination for internal friction angle, $\varphi = 30^0$, $\delta = \varphi/2$ and with $k_v = 0.5k_h$, $k_h = 0.2$. is presented in Fig. 5. It is seen that seismic active earth pressure increases as the backfill surface inclination increases.

5. Comparison of results

A typical comparison of normalized pressure distribution behind rigid wall obtained by the present study with that by Mononobe-Okabe method for the cases of $k_v = 0.5k_h$, $k_h = 0.1$, $\varphi = 30^0$, $\delta = \varphi/2$, $H/\lambda_s = 0.3$, $H/\lambda_p = 0.16$ with 20^0 backfill surface inclination is shown in Fig. 6. It reveals non-linear seismic active earth pressure distribution in a more realistic manner as compare with the pseudo-static method.

The basic Eq. (12) also clearly shows mathematically the non-linearity of the seismic active earth

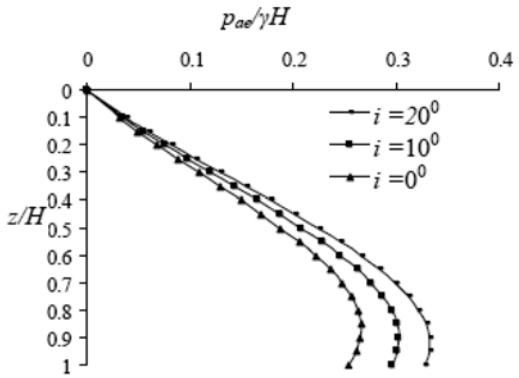

Fig. 5 Variation of normalized pressure distribution with backfill surface inclination

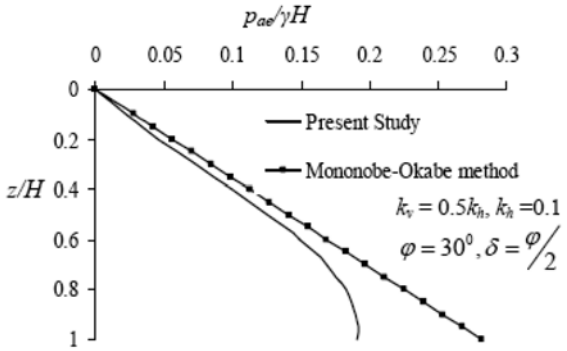

Fig. 6 Typical comparison of normalized pressure distribution by present study with Mononobe-Okabe method

pressure distribution. Fukuoko and Imamura (1984) made a number of research work on prototype retaining walls constructed at mountainous roads to investigate the distribution of dynamic earth pressure. It was observed from the test result that distribution of changing in earth pressure on the back of the retaining wall was not a triangular shape. Moreover the fluctuation of earth pressure distribution was larger than the lower part. The reported published data for prototype retaining wall under earthquake condition by Fukuoka and Imamura (1984) and the centrifuge experimental results for model retaining wall under seismic condition measured by Steedman and Zeng (1990) had shown clearly the non-linear variation of the normalized seismic active earth pressure with depth of the wall confirms the present findings.

6. Conclusions

The pseudo-dynamic method of analysis, presented in the present paper, considers the effect of time and phase change in shear and primary waves propagating in the backfill behind the rigid wall. This provides more realistic non-linear seismic active earth pressure distribution behind the retaining wall as compared to the Mononobe-Okabe method using pseudo-static approach. Non-linearity of the active earth pressure distribution increases with increase in the seismicity which leads to the shifting of point of application of total thrust required for the design purpose. However, the conventional pseudo-static approach provides only linear earth pressure distribution irrespective of static and seismic condition leading to a major drawback in design criteria. The seismic active earth pressure distribution and as well as the total active thrust behind the rigid wall is obtained by considering the wall friction, backfill surface inclination, horizontal and vertical earthquake accelerations. It is found that magnitude of seismic active earth pressure increases with the increase in the values of horizontal and vertical seismic acceleration but decreases with increase in the value of soil friction. The seismic active earth thrust is highly sensitive to the friction angle of the soil and comparatively less sensitive to the wall friction angle. Backfill surface inclination affects significantly the magnitude of active earth pressure and increases with the increase of inclination.

References

Choudhury, D. and Nimbalkar, S. (2005), "Pseudo-dynamic approach of seismic active earth pressure behind retaining wall", *J. Geotech. Geological Eng.*, **24**, (5), 1103-1113.

Choudhury, D. and Nimbalkar, S (2006), "Seismic passive resistance by pseudo-dynamic method", *Geotechnique*, **55**, (9)**,** 688-702.

Das, B.M. (1993), *Principle of soil dynamics*, Boston, Massachusette: PWS-KENT Publishing Company.

Fukuoka, M. and Imamura, Y. (1984), "Researches on retaining walls during earthquakes", *Proceedings Eight World Conference on Earthquake Engineering*, San Francisco, USA, Vol. 3, 501-508.

Ghosh, S. (2007), "Seismic passive earth pressure behind non-vertical retaining wall using pseudo-dynamic analysis", *J. Geotech. Geological Eng.*, **25**, (6), 693-703.

Ghosh, S., Dey, G.N. and Datta, B. (2008), "Pseudo static analysis of rigid retaining wall for dynamic active earth pressure", *Proceeding of the 12th International Conference of International Association for Computer Methods and Advances in Geomechanics*, Goa, India, 4122-4131.

Ghosh, S. (2010), "Seismic active earth pressure coefficients on battered retaining wall supporting inclined c-φ backfill", *Indian Geotech. J.*, **40**, 178-183.

Ghosh, S. and Saran, S.K. (2010), "Graphical method to obtain dynamic active earth pressure on rigid retaining wall supporting c-φ backfill", *EJGE*, **15**, Bund D, 1-5.

Mononobe, N. and Matsuo, H. (1926), "On the determination of earth pressure during earthquakes", *Proceedings of the World Engineering Conference*, **9**, 176.

Okabe, S. (1926), "General theory of earth pressure", *J. - JSCE*, **12**(1).

Richards, R., Elms, D.G. and Budhu, M. (1990), "Dynamic fluidization of soil", *J. Geotech. Eng. - ASCE*, **110**, 740-759.

Saran, S. and Gupta, R.P. (2003), "Seismic earth pressure behind retaining walls", *Indian Geotech. J.*, **33** (3)**,** 185-213.

Soubra, A.H. (2000), "Static and seismic passive earth pressure coefficients on rigid retaing structures", *Can. Geotech. J.*, **37**, 463-478.

Steedman, R.S. and Zeng, X. (1990), "The influence of phase on the dilution of pseudo-static earth pressure on a retaining wall", *Geotechnique*, **40**(1), 103-112.

GM

Nomenclature

$a_h(z,t)$	: horizontal earthquake acceleration at any depth z and at any time t (m/s^2)
$a_v(z,t)$	: vertical earthquake acceleration at any depth z and at any time t (m/s^2)
H	: height of the retaining wall (m)
i	: backfill surface inclination (degree)
$P_{ae}(t)$	: earth pressure in active state at any time t (kN/m^2)
ρ	: density of soil mass (kg/m^3)
γ	: unit weight of soil mass (kN/m^3)
m	: mass of failure soil wedge (kg)
W	: total weight of soil wedge (kN)
φ	: soil friction angle (degree)
δ	: angle of wall friction (degree)
k_h, k_v	: horizontal and vertical seismic coefficients respectively
α	: angle of wedge surface with horizontal (degree)
G	: shear modulus of the backfill soil material (kN/m^2)
ν	: poisson's ratio of backfill soil material
V_s, V_p	: shear wave and primary wave velocity in the backfill material (m/s)

t, T, ω : any time t within the time period T moving at an angular velocity ω (s, rad/s)
$Q_h(t)$: total horizontal seismic inertia force acting at the *cg* of the wedge (kN)
$Q_v(t)$: total vertical seismic inertia force acting at the *cg* of the wedge (kN)
λ_s : wave length of shear wave (m)
λ_p : wave length of primary wave (m)
K_{ae} : total seismic earth pressure coefficient due to the combination of k_h and k_v